

Tunable, long-wavelength PtSi/SiGe/Si Schottky diode infrared detectors

J. R. Jimenez^{a)}

Faura Scientific, Inc., Bedford, Massachusetts 01730

X. Xiao^{b)} and J. C. Sturm

Department of Electrical Engineering, Princeton University, Princeton, New Jersey 08544

P. W. Pellegrini

Rome Laboratory, Hanscom Air Force Base, Massachusetts 01731

(Received 9 March 1995; accepted for publication 31 May 1995)

We have fabricated *p*-type PtSi/SiGe/Si Schottky diodes with barrier heights (from photoresponse) that are lowered (relative to PtSi/Si) and highly dependent on the applied bias. The variability in the barrier height is obtained by using the SiGe/Si valence band offset as an additional barrier. When placed in close proximity to the PtSi/SiGe Schottky barrier, the total effective barrier can be altered dramatically by adjusting the applied reverse bias. The voltage sensitivity of the total barrier height can be controlled by the SiGe layer thickness. The voltage-variable barrier heights range, for example, from 0.30 eV at zero bias to 0.12 eV at 2.4 V reverse bias for a 20%, 450 Å thick SiGe layer. This lowest barrier height corresponds to a cutoff wavelength of 10 μm, extending the detection range of PtSi infrared detectors to the long-wavelength range. The quantum efficiency coefficients C_1 are normal at this long-wavelength end, but reduced over the rest of the tunable range, because hot carriers have to traverse the entire SiGe thickness in order to be detected. The hot carriers' energy losses from quasielastic scattering in the SiGe are taken into account in a theoretical model that gives good agreement with data. © 1995 American Institute of Physics.

PtSi/Si Schottky diodes are currently used in commercially available infrared video cameras for imaging at wavelengths below 5.5 μm.¹ This cutoff wavelength is defined by the PtSi/*p*-Si Schottky barrier height (SBH) of ~0.22 eV. It is desirable to extend Si-based infrared detectors to longer wavelengths (up to 12 μm). Long-wavelength Si-based infrared detectors that have been demonstrated include IrSi/Si Schottky diodes² (SBH ~0.12 eV), SiGe/Si heterojunction internal photoemission (HIP) detectors,³ SiGe/Si quantum well infrared photodetectors (QWIPs),^{4,5} and doping-spike PtSi/Si detectors.⁶ Recently, PtSi/SiGe Schottky diodes were reported with extended cutoff wavelengths of up to 8.5 μm for 15% Ge.^{7,8} While the extension of cutoff wavelengths has been the motivation for silicide/SiGe detectors, another useful effect, that of highly voltage-variable barrier heights, can be obtained by using the SiGe/Si valence band offset in conjunction with the PtSi/SiGe Schottky barrier. For thin SiGe layers, the SiGe/Si offset can be made to lie in the diode's depletion region, just behind the Schottky barrier maximum, and extending higher in (hole) energy. Because the offset barrier is deeper in the semiconductor than the Schottky barrier, it is much more susceptible to an applied reverse bias. Such voltage tunable, extended-wavelength PtSi/SiGe/Si diodes are the subject of this letter. (A different type of tunable infrared detector, based on the growth of Si on epitaxial silicides or degenerately doped SiGe, has been previously reported.^{9,10})

The *p*-type (boron-doped) SiGe structures were grown on high-quality *p*-Si substrates by rapid thermal chemical

vapor deposition (RTCVD), in a system that has been described previously.¹¹ The SiGe layers were capped with Si, and a layer of graded Ge concentration was grown between the SiGe and the Si. SiGe samples with Ge concentrations of 10%, 15%, and 20% were used in this study, together with a control PtSi/Si diode. To keep the layers strained, the thicknesses were reduced with increasing Ge content. Thus the total SiGe layer thicknesses were 1200, 650, and 500 Å, respectively. The portions of the total SiGe layer thickness with uniform (nongraded) Ge concentrations were 600, 400, and 300 Å, respectively. The PtSi diodes were made by reacting Pt with the Si capping layer. This was done to avoid Pt–SiGe reactions, which have been observed to result in barrier heights that are higher than PtSi/Si.^{7,12} The Pt depositions were done by electron beam evaporation in a load-locked ultrahigh vacuum system. The wafers were held at 350 °C during deposition and the silicides were formed by annealing *in situ* for 1 h. The samples were processed with guard ring structures in the Si below the SiGe. Absolute photoresponse measurements were made with a Perkin Elmer single-pass monochromator and a SiC globar at 1000 °C as the infrared source. The input radiation was chopped at 139 Hz and the photoresponse measured by lock-in amplifier. Measurements were made at a temperature of 40 K or lower. Low temperatures are necessary to minimize the thermally generated current, compared with the photocurrent.

Figure 1 is a band diagram of a tunable PtSi/SiGe/Si Schottky diode detector, showing the extra barrier formed by the SiGe/Si offset at zero bias. The effective barrier height to photoexcited holes is increased and is given by the height of this offset peak above the Fermi level. As the externally applied reverse bias is increased, the SiGe/Si offset barrier is lowered in (hole) energy much more than the Schottky bar-

^{a)}Electronic mail: jjimenez@emerald.tufts.edu

^{b)}Present address: Intel Corporation, MS RN3-21, 2200 Mission College Blvd., Santa Clara, CA 95052.

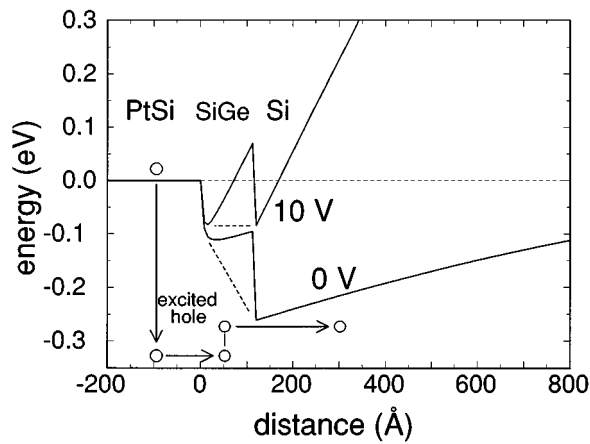


FIG. 1. Calculated valence band diagram of a PtSi/SiGe/Si structure at 0 and 10 V reverse bias, for 10^{16} cm^{-3} B doping and 120 Å of $\text{Si}_{0.8}\text{Ge}_{0.2}$. The dashed line is the valence band edge if part of the Si is replaced by a layer of linearly graded Ge concentration.

rier. The result for a PtSi/SiGe/Si structure is a composite barrier, Schottky plus heterojunction, whose total height is much more susceptible to a reverse bias than a normal Schottky barrier. This enhanced variability, however, holds only up to a transition point voltage, when the SiGe/Si offset is lower than the Schottky barrier. At voltages greater than this transition voltage, the dependence of the barrier height is that of a standard Schottky diode.

Figure 2 is a series of Fowler plots of the quantum efficiency of the PtSi/ $\text{Si}_{0.85}\text{Ge}_{0.15}$ /Si diode at various reverse biases. At low biases, high barrier heights, corresponding to emission over the SiGe/Si offset, are observed. These barrier heights change rapidly with bias, which is expected for emission over the SiGe/Si offset. The energy loss due to scattering of hot carriers in the SiGe will result in some deviation of the Fowler plot from linearity near the threshold, so that the linearly extrapolated barrier heights will be somewhat greater than the height of the SiGe/Si offset. After about 0.6

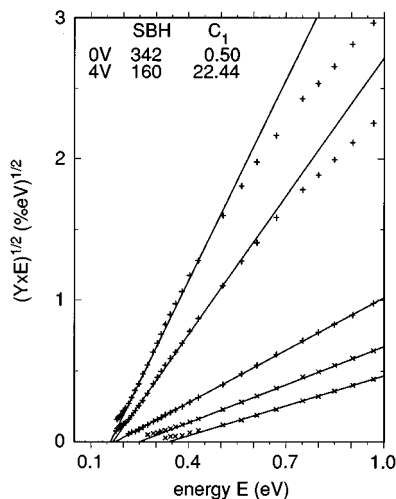


FIG. 2. Fowler plots of the quantum efficiency of a PtSi/ $\text{Si}_{0.85}\text{Ge}_{0.15}$ /Si diode at 0, 0.4, 0.6, 1.0, and 4.0 V of reverse biases. SBH values are in meV, and C_1 values are in %/eV. Plots at other intermediate biases are not shown to prevent clutter.

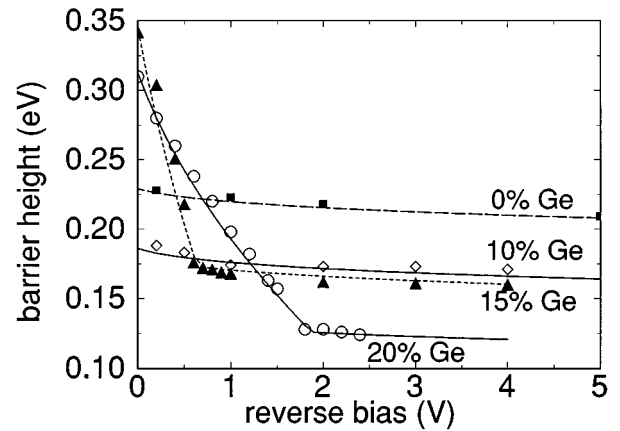


FIG. 3. Schottky barrier heights obtained from Fowler plots, vs reverse bias, for a series of PtSi/SiGe/Si diodes of various Ge contents. The solid lines are for theoretical fits, with parameters $z_{sg}=450 \text{ Å}$, $\epsilon_{\text{loss}}=103 \text{ meV}$, and $N_a=6.5 \times 10^{15} \text{ cm}^{-3}$ for 20% Ge, and $z_{sg}=650 \text{ Å}$, $\epsilon_{\text{loss}}=210 \text{ meV}$, and $N_a=1.3 \times 10^{16} \text{ cm}^{-3}$ for 15% Ge.

V, the barrier heights change much more slowly, which is expected for emission over the Schottky barrier.

Figure 3 is a plot of the barrier heights against reverse bias, obtained from the Fowler plots in Fig. 1 and from other samples of varying Ge concentrations and thicknesses. For the 20% and 15% Ge samples, the SiGe thicknesses and band offsets are such that the large bias dependence of emission over the SiGe/Si offset is observed, followed by the normal Schottky bias dependence after a transition-point bias. Note that a saturation barrier height of 0.12 eV is measured for the $\text{Si}_{0.8}\text{Ge}_{0.2}$ sample, corresponding to a cutoff wavelength of 10 μm . For the 10% Ge sample, the total SiGe layer was thick enough so that no second barrier was detected, and only the normal Schottky bias dependence is observed, similar to that in the 0% Ge sample. It must be noted that the maximum height of the SiGe offset barrier depends only on the initial Ge concentration at the PtSi/SiGe interface and on the thickness of the total SiGe layer, and not on the rate of Ge grading within the layer. The Ge grading affects only the profile of the energy barrier.

The bias-dependent effective barrier heights are modeled by modifying the standard Schottky barrier equation.¹³ For metal/SiGe/Si diodes in which the SiGe is thin enough to lie entirely within the depletion region, the effective barrier height $q\phi_{\text{eff}}$, for p -type diodes, will be¹⁴

$$q\phi_{\text{eff}} = -U\{z_{sg}, W[V, V_{bi}(\phi_{sg}, \Delta E_v)]\} + \frac{q^2}{16\pi\epsilon z_{sg}} + q\phi_{sg} + \Delta E_v + \epsilon_{\text{loss}}, \quad (1)$$

where z_{sg} is the thickness of the SiGe layer, and ΔE_v is the valence band offset at the SiGe/Si interface, taken as 90% of the total band gap change ΔE_g , for which the empirical equation $\Delta E_g = 0.94x - 0.43x^2 + 0.17x^3$, where x which is the Ge percentage, was used.¹⁵ All energies are referred to the Fermi level E_F . The second term in Eq. (1) is the image potential energy, and $q\phi_{sg}$ is the PtSi/SiGe Schottky barrier height. In the first term, $U(z, W)$ is the electrostatic potential energy due to the space charge region

($U > 0$ for holes), $W(V, V_{bi})$ is the depletion layer width, V is the externally applied bias, and $V_{bi}(\phi_{sg}, \Delta E_v)$ is the built-in potential difference. For the metal/SiGe/Si diode, again where the SiGe is thin enough to be completely depleted, the built-in potential, difference is modified by the addition of the valence band offset: $qV_{bi} = q\phi_{sg} + \Delta E_v - (E_v^\infty - E_F)$, where the last term in the parentheses is determined by the doping level. From this V_{bi} , U and W are calculated in the standard way.¹³ The last term in Eq. (1) must be included because the expected energy loss of carriers from scattering in the SiGe will result in an effectively higher threshold energy for hot carriers from the metal. This energy loss is depicted schematically in Fig. 1. The energy loss scattering mechanism must have low momentum transfer so that carriers are not redirected away. A likely mechanism is therefore optical phonon scattering from the three optical modes in SiGe. The resulting fits are the solid curves in Fig. 3. For 20% Ge, the parameters of the curve are $z_{sg} = 450 \text{ \AA}$, $\epsilon_{\text{loss}} = 103 \text{ meV}$, and $N_a = 6.5 \times 10^{15} \text{ cm}^{-3}$. For 15% Ge, the parameters of the curve are $z_{sg} = 650 \text{ \AA}$, $\epsilon_{\text{loss}} = 210 \text{ meV}$, and $N_a = 1.3 \times 10^{16} \text{ cm}^{-3}$. The values of ϵ_{loss} , comparable in magnitude to the other large terms in Eq. (1), indicate that several phonon scattering events occur in the SiGe before emission over the SiGe/Si barrier. This is a result of the thickness of the SiGe layer. The value of ϕ_{sg} is determined by the saturation value and is not adjustable.

Analysis of the bias dependence of C_1 , obtained from the slope of the Fowler plots, shows behavior that is consistent with emission over the SiGe/Si interface. For normal Schottky diodes C_1 has been shown to depend on $z_m(V)$, the bias-dependent position of the Schottky barrier maximum, typically about 25–50 Å from the metal-semiconductor interface.¹⁶ The bias dependence is found to be proportional to $\exp[-z_m(V)/L]$, where L is a composite length for scattering events that prevent carriers that have crossed the metal-semiconductor interface from surmounting the Schottky barrier maximum. This length therefore includes elastic scattering events that redirect carrier momenta, as well as completely inelastic scattering events, so that it is to be distinguished from semielastic (i.e., with some energy loss) scattering lengths deduced from the last term of Eq. (1). A log plot of C_1 vs z_m (z_m is calculated from the reverse bias) should therefore yield approximately linear behavior, as observed in Fig. 4 for the PtSi/Si control diode and the 10% Ge sample, in which the barrier heights had normal Schottky bias dependence. For PtSi/SiGe/Si diodes, the C_1 coefficients at low bias are expected to be very much reduced, because the much greater distance is associated with emission over the SiGe/Si interface, as compared to $z_m(V)$. Around the transition-point bias, however, the C_1 coefficient should rise sharply to much higher values, corresponding to emission over the Schottky barrier. This behavior can be observed in Fig. 2, where the slopes corresponding to the rapidly changing barrier heights are much smaller than the slopes corresponding to the slowly changing barrier heights. It is also made clearer in Fig. 4, for the 15% and 20% Ge samples. In this plot, the low values for emission over the SiGe/Si offset are followed by a rapid rise and subsequent linear behavior.

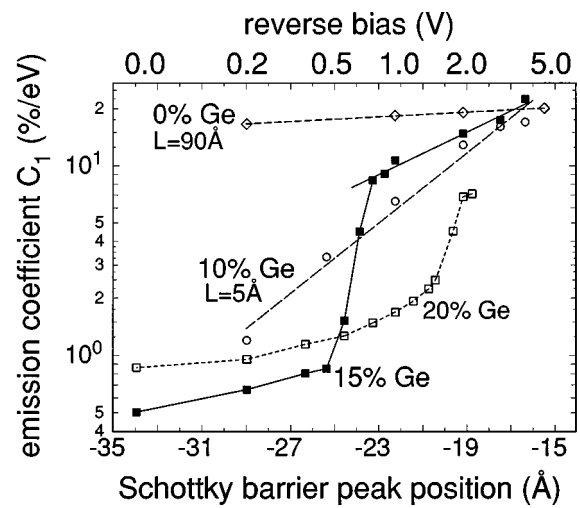


FIG. 4. Quantum efficiency coefficients C_1 obtained from the Fowler plots, as a function of distance of the Schottky barrier maximum from the PtSi for a series of samples of varying Ge concentration. The distances are calculated, for 10^{16} cm^{-3} B doping, from the reverse bias, which is shown on the upper horizontal scale.

The tunability feature should allow for spectral analysis of infrared images by varying the spectral response from frame to frame.

We would like to acknowledge the measurement work of Melanie M. Weeks, discussions with Dr. Jonathan M. Mooney, and Pt depositions at the David Sarnoff Research Center. Parts of this work were supported by the National Science Foundation, the Office of Naval Research, and the Air Force Office of Scientific Research.

- ¹ For recent reviews, see F. D. Shepherd, Proc. SPIE **1735**, 250 (1992) and W. F. Kosonocky, Proc. SPIE **1308**, 2 (1990).
- ² P. W. Pellegrini, A. Golubovic, C. E. Ludington, and M. M. Weeks, Tech. Dig. Int. Electron. Device Mtg. 157 (1982).
- ³ T. L. Lin, A. Ksendzov, S. M. Dejewski, E. W. Jones, R. W. Fathauer, T. N. Krabach, and J. Maserjian, IEEE Trans. Electron Devices **38**, 1141 (1991).
- ⁴ R. People, J. C. Bean, C. G. Bethea, S. K. Spitz, and L. J. Peticolas, Appl. Phys. Lett. **61**, 1122 (1992).
- ⁵ R. P. G. Karunasiri, J. S. Park, and K. L. Wang, Appl. Phys. Lett. **61**, 2434 (1992).
- ⁶ T. L. Lin, J. S. Park, T. George, E. W. Jones, R. W. Fathauer, and J. Maserjian, Appl. Phys. Lett. **62**, 3318 (1993).
- ⁷ X. Xiao, J. C. Sturm, S. R. Parihar, S. A. Lyon, D. Meyerhofer, S. Palfrey, and F. V. Shallcross, IEEE Electron Device Lett. **EDL-14**, 199 (1993).
- ⁸ X. Xiao, J. C. Sturm, S. R. Parihar, S. A. Lyon, D. Meyerhofer, and S. Palfrey, Tech. Dig. Int. Electron. Device Mtg. 125 (1992).
- ⁹ I. Sagnes, C. Renard, and P. Badoz, J. Phys. **IV**, C6–139 (1994).
- ¹⁰ L. Pahun, Y. Campidelli, F. A. d'Avitaya, and P. A. Badoz, Appl. Phys. Lett. **60**, 1166 (1992).
- ¹¹ J. C. Sturm, P. V. Schwartz, E. J. Prinz, and H. Manoharan, J. Vac. Sci. Technol. B **9**, 2011 (1991).
- ¹² J. R. Jimenez, X. Xiao, J. C. Sturm, P. W. Pellegrini, and M. M. Weeks, J. Appl. Phys. **75**, 5160 (1994).
- ¹³ S. M. Size, *Physics of Semiconductor Devices* (Wiley, New York, 1981), Chap. 5.
- ¹⁴ For a more detailed discussion, see J. R. Jimenez, X. Xiao, J. C. Sturm, P. W. Pellegrini, and M. M. Weeks, Proc. SPIE **2225**, 393 (1994).
- ¹⁵ J. C. Bean, Proc. IEEE **80**, 571 (1992).
- ¹⁶ J. M. Mooney, J. Appl. Phys. **65**, 2869 (1989).